Research on Stator and Rotor Meshing Simulation Model of Screw Motor

Yuchun Kuang [a], Yijia He, Cong Zhang, Longmei Wu

School of Mechatronic Engineering, Southwest Petroleum University, Chengdu, Sichuan 610500, PR China

[a]765151413@qq.com

Abstract

Screw drilling tool is a kind of downhole power tool widely used in petroleum drilling engineering. The core power component of screw drilling tool is motor, which is composed of stator and rotor. This paper ignores the dynamics and other factors, but only considers the impact of contact force on the rotor. In addition, the stator and rotor meshing model is established, to make the rotor in theoretical balanced state when it is rotating inside the stator. On basis of this, the magnitude of interference between the stator and the rotor is defined.

Keywords

Screw Drilling Tool, Stator And Rotor Meshing Model, Magnitude of Interference.

1. Introduction

Because the stator lining is rubber material, belonging to elastomer, it is in need of certain magnitude of interference between rotor and stator. And when the contact stress caused by magnitude of interference is larger than pressure differential between adjacent volume cavity, it can ensure the motor good sealing performance, and further ensure the motor good output performance. Due to the existence of magnitude of interference, the stator and the rotor will generate several contact areas, thereby producing several contact forces acting on the rotor. Under actual working condition, due to the effect of several contact forces, the trajectory of rotor center will deviate from the theoretical center trajectory, together with complex frictional resisting moment, inertia force, pressure deviation caused by dynamic change of seal cavity and other complicated factors impact, the actual motion center trajectory of the rotor is difficult to determine. Finally the center trajectory of the rotor is no longer a circle regarding eccentric distance e as radius, thus the actual magnitude of interference and theoretical magnitude of interference also produce differences. That is why the magnitude of interference between the rotor can not be accurately described under theoretical condition, so more reasonable stator and rotor meshing model is necessary to describe the magnitude of interference between the two. This paper only considers the influence of contact forces, and ignores the influence of rotor dynamics, so a meshing simulation model of stator and rotor is established.

2. Contact model of stator and rotor

The rotor is made of steel material, whose surface is electroplated with a layer of chromium material, to increase its abrasive resistance. The stator consists of stator steel tube and rubber closely attaching to its inner wall. The rubber is made of hyperelastic material, and two parts meshing model, which can be simplified as the situation [1-5] that the absolute rigid cylinder under plane strain state contacts elastomer.

The contact area of stator (①) and rotor (①) is as shown in Fig. 1. This kind of contact is called internal contact, whose curvature radius is respectively R_1 and R_2. The solid line represents the contact boundary before deformation, while the dotted line represents the contact boundary after deformation. When it happens to have no contact force between the two, only contact at one point *O*; under the effect of pressure *P*, *O* point moves to O 'point, and the contact width becomes $2a$. Take

M_1 and M_2 two points in two curves r away from the common normal line. Before elastic deformation, the gap between the two points is（L_2-L_1）, as shown in Fig. 2, according to the geometric relationship [6]:

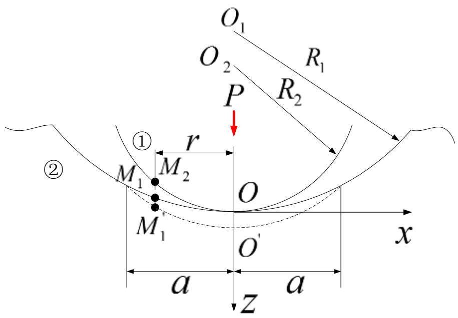

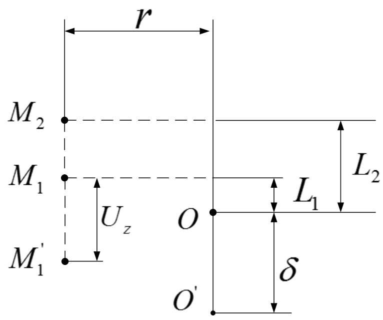

Fig. 1 Schematic diagram of contact area Fig. 2 Deformation relation of contact area

$$L_1 = \frac{r^2}{2R_1}, L_2 = \frac{r^2}{2R_2} \tag{1}$$

$$L_2 - L_1 = \frac{r^2}{2R_2} - \frac{r^2}{2R_1} = \frac{R_1 - R_2}{2R_1R_2} r^2 \tag{2}$$

Due to elastic deformation, the displacement that rotor moves along the Z direction is δ. At the same time, M_1 point moves down to the new point, namely M_1'. Its deformation is U_z, and coincident with M_2 in contact area. According to the geometric relationship:

$$\delta = U_z + (L_2 - L_1) \tag{3}$$

Thus, the deformation of each point in contact area can be obtained:

$$U_i = \delta - (\mathrm{L}_2 - \mathrm{L}_1) = \delta - \frac{R_1 - R_2}{2R_1R_2} r^2, (\mathrm{r} \le a) \tag{4}$$

When r equals to a, located at the boundary of contact area, the deformation of the elastomer approximately equal to zero, that is, U_{i} approximates 0; to obtain:

$$\delta = \frac{R_1 - R_2}{2R_1R_2} a^2 \tag{5}$$

According to the literature [7], the contact pressure P on per unit length can be:

$$P = \frac{\pi E \delta}{2(1-\nu^2)\ln\dfrac{H}{2R^*\delta} + (3-4\nu)(1+\nu)} \tag{6}$$

Here, $1/R^* = 1/R_2 - 1/R_1$, E, ν respectively represent the elasticity modulus and Poisson's ratio of stator rubber material; H represents the thickness of rubber at contact point.

If the stator and rotor contact outside, it is available to just assign negative value to R_1 in above formula. If the contact area is close to a straight line, the curvature radius of the stator is larger, which can order R_1 to tend to positive infinity.

2.1 Computing method of resultant force in contact force system

The stator and the rotor will match up to produce a number of contact areas, each contact area will generate contact force F_i of different size and direction, as shown in Fig. 3.

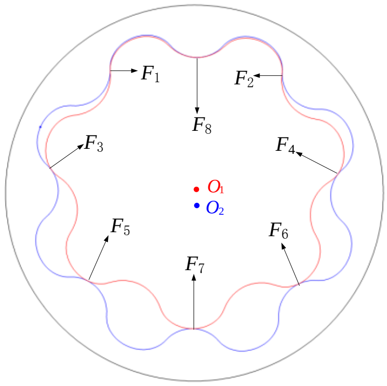

Fig. 3 Schematic diagram for contact force system acting on rotor

In order to obtain the resultant force in contact force system, according to the translation theorem[8] of force in theoretical mechanics. First of all, each contact force F_i needs to be translated to rotor center O_1, also need to attach corresponding couple M_i, the couple moment is equal to the moment that original force F_i acts on rotor center O_1. As shown in Fig. 4.

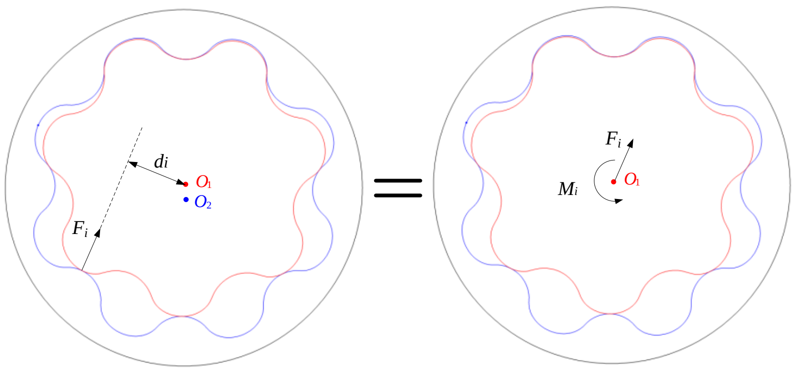

Fig. 4 Translation schematic diagram of force

The contact force system and the couple system translated to rotor center are called planar force system and planar couple system concurrent in rotor center, as shown in Fig. 5. According to the analytical method synthesized by planar concurrent force system, the resultant force F_R of concurrent force system can be obtained. The establishment of rectangular coordinate system O_1xy, as shown in Fig. 6. The analytical expression for the resultant force F_R of concurrent force system is:

$$F_R = F_{Rx} + F_{Ry} = F_x \vec{i} + F_y \vec{j} \tag{7}$$

In the formula, F_x, F_y represent the projection of resultant force F_R in the X, Y axis projection, according to Fig. 6:

$$F_x = F_R \cos\theta, F_y = F_R \cos\beta \tag{8}$$

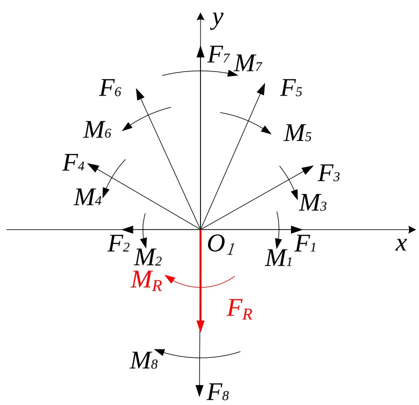

Fig.5 Planar force system and planar couple system concurrent in rotor center

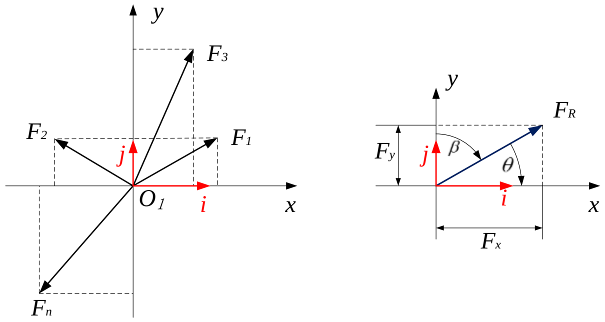

Fig. 6 The analytical expression for the resultant force FR of concurrent force system

According to resultant vector projection theorem, the projection of resultant vector on one certain axis is equal to the algebraic sum of the projection of each sub vector on the same axis.

$$\begin{cases} F_x = F_{x1} + F_{x2} + \cdots + F_{xn} = \sum_{i=1}^{n} F_{xi} \\ F_y = F_{y1} + F_{y2} + \cdots + F_{yn} = \sum_{i=1}^{n} F_{yi} \end{cases} \tag{9}$$

Here, F_{x1} and F_{y1} , F_{x2} and F_{y2} $\cdots$, F_{xn} and F_{yn} respectively represent the projection of each component force in x axis and y axis.

The size and direction of the resultant force is:

$$\begin{cases} F_R = \sqrt{F_x^2 + F_y^2} = \sqrt{(\sum F_{xi})^2 + (\sum F_{yi})^2} \\ \cos(\vec{F_R}, \vec{i}) = \frac{F_x}{F_R} = \frac{\sum F_{xi}}{F_R} \\ \cos(\vec{F_R}, \vec{j}) = \frac{F_y}{F_R} = \frac{\sum F_{yi}}{F_R} \end{cases} \tag{10}$$

Any couple in the same plane can be synthesized into one resultant couple, resultant couple moment M_R is equal to algebraic sum of every moment of couple:

$$M_R = \sum_{i=1}^{n} M_i \tag{11}$$

2.2 Rotor balance calculation

It is knowable from above that, when the rotor goes on uniform rotation, the resultant moment M_R generated by the contact force system acting on the rotor, and torque and the contact resultant force generated by the differential pressure of volume cavity make the rotor in a state of equilibrium. In this paper, the influence of the rotor dynamic factor is neglected, and the influence of the contact force produced in rotor contact area on the rotor position is considered. When the rotor is in different positions, if the contact resultant force is not zero, then the rotor will drive the rotor under the effect of resultant force and along the direction of resultant force. The rotor will not be in balance until the force is zero or minimum. Thus, in the premise of contact resultant force balance, the paper adopts repeated iteration method, to get the balance state and rotor center position of the rotor. The rotor revolution angle varies from 0 degree to 360 degrees, and the center position of the rotor in balance is calculated every 5 degree, further to get the movement locus of rotor center .

An excellent iterative algorithm can accelerate the convergence speed and improve the computational efficiency. The basic idea of iterative optimization algorithm is:

(1) Given an initial point x_0 .

(2) According to a certain iterative rule, produce a point range $\{x_k\}$, so that:

When $\{x_k\}$ is a finite point range, the last point is the optimal solution of the optimization model question.

When $\{x_k\}$ is an infinite point range, its limit point is the optimal solution

When it is infinite point column, its limit point is the optimal solution.

In this paper, in obtaining the balanced state of the rotor at any time, after several improvements, the following balanced iterative algorithm is put forward. The force acting on the contact force of the rotor has a great relation with the position of the rotor center, taking the resultant force of the contact force system as the objective function,

$$\min F_R = f(x_c, y_c) \tag{12}$$

Among which, xc and yc are the center of the rotor.

Constraint conditions are:

$$F_{R(k+1)} < F_{R(k)} \tag{13}$$

The initial value of the rotor center is x0, y0, and the initial contact force FR (0) in the initial state is calculated and the initial directions of its resultant force are obtained as Nx0, Ny0. Set the step length dk and step length factor α_k to make the rotor center position move along the direction of force, and the formula is:

$$\left.\begin{aligned} X_{k+1} &= X_k + \alpha_k d_k N_{x(k)} \\ Y_{k+1} &= Y_k + d_k N_{y(k)} \end{aligned}\right\} \tag{14}$$

The above steps should be repeated until the iteration is stopped, $\min F_R$ satisfies the termination condition and the approximate optimal solution.

The stator-rotor meshing and its iterative algorithm flow diagram is shown in Fig. 7.

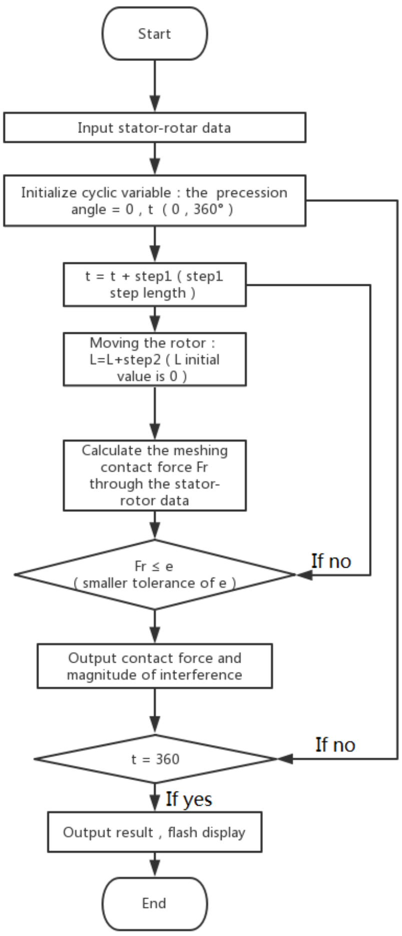

Fig. 7 Stator-rotor Meshing and Its Brief Equilibrium Algorithm Flow Diagram

3. Comparison of Numerical Results

When the rotor is doing theoretical planetary motion inside the stator, the rotor is in a non-equilibrium state due to the influence of contact force and so on and the center of the rotor takes certain force. At first, the meshing simulation model established in this dissertation is used to calculate the force at the rotor center in different precession angle, and meanwhile, using the ANSYS to carry out numerical calculation to simulate the theoretical planetary motion done by the rotor inside the stator and obtain the force at the rotor center. Finally, the results obtained by the two methods are compared.

Since the theoretical equilibrium state of the rotor at different moments in the process of rotor rotation which refers to the force at the rotor center is theoretically being zero can be obtained through the motor stator-rotor meshing model, and in order to validate that the meshing model can effectively obtain the equilibrium state of the rotor, the ANSYS model is used again to obtain the central force of the rotor in the theoretical equilibrium state.

3.1 The Ideal Planetary Motion Made by the Rotor

When the rotor rotates 5 °per revolution, the translational degree of freedom of the outer node of the stator rubber and the center point of the rotor is completely constrained. The constraint force of the rotor center, in other words, the resultant force of the rotor at this time is calculated and extracted.

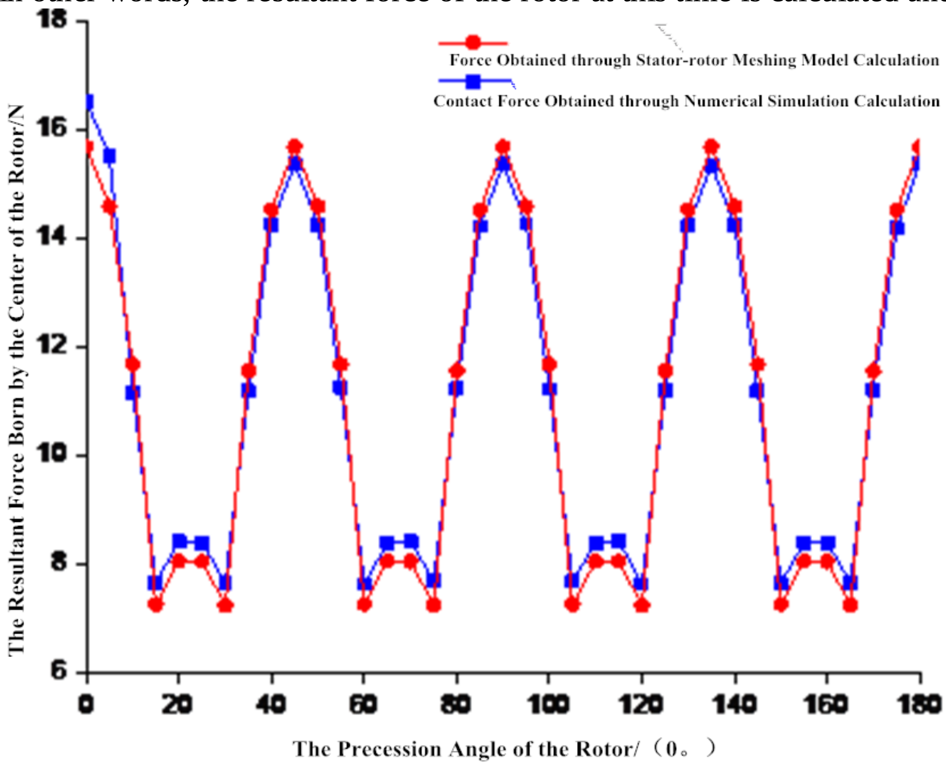

Fig. 8 The Comparison between Contact Force Obtained through Numerical Calculation and Meshing Model Calculation

Obtain the contact force acting on the center of the rotor at different moments when the rotor is rotating and compare with the one calculated by the meshing model. Figure 8 shows that the contact force calculated by the meshing model is close to that of the numerical simulation, and the trend is also very consistent which proves that the method of calculating the force acting on the rotor center by the established stator-rotor contact model has a certain degree of rationality.

3.2 The Planetary Motion in the Equilibrium State of the Rotor

In this paper, the meshing simulation model is established to obtain the position of the equilibrium state of the rotor at different moments during the rotation process, and input the shape of the rotor in the theoretical equilibrium state into the ANSYS to calculate the rotor’s center force so as to verify whether the force in the center of rotor is zero or relatively small, in other words, the rotor is in equilibrium.

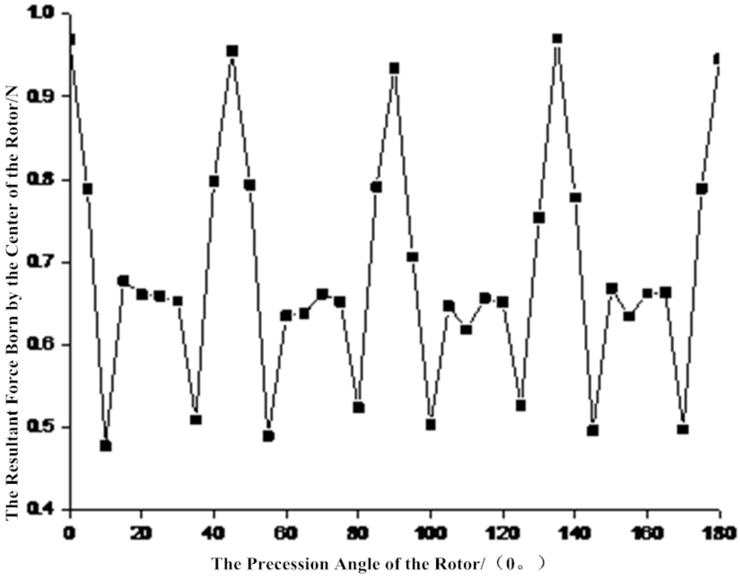

Fig. 9 The Resultant Force Born by the Rotor Center in Equilibrium

From Fig. 9, it is found that the contact force acting on the center of the rotor is less than 1N by simulating the balanced motion of the rotor through ANSYS. Compared to the resultant force born by the rotor under the ideal planetary motion in Fig. 8, the force in equilibrium is significantly reduced which proves that the method of calculating the rotor equilibrium state by the simulation model of the rotor-stator meshing established in this paper has certain reasonableness.

4. Conclusion

The magnitude of interference between the stator and rotor of the screw motor have a great impact on the sealing performance and output performance of the motor. Setting a reasonable magnitude of interference between the stator and rotor is of great application significance in ensuring the sealing performance and improving the output performance of the motor. In this chapter, by ignoring the liquid pressure, centrifugal force and other dynamic factors, simulation model of meshing rotor is established, in which the rotor in any precession angle and theoretically equilibrium inside the stator, then the maximum magnitude of interference at the contact area of one head of the rotor and a stator rubber is taken as the rotor magnitude of interference at this angle, and by comparing with finite element method fem analysis results, the meshing model has certain rationality, which has laid the foundation for the subsequent design of the reasonable magnitude of interference between the stator and rotor.

References

[1] Yen-Hung Chen, Yuan-Shin Lee, Shu-Cherng Fang. Optimal cutter selection and machining plane determination for process planning and NC machining of complex surfaces [J]. Journal of Manufacture Systems, 1988, 17(5).

[2] M.S.Delpassand. Stator life of a Positive Displacement Downhole Drilling Motor[J].Transactions of the ASME,1999,121:110-116

[3] Azar Azizov, Karl Hilthon , Fadi Mounzer . Design of New Fit-For-Purpose Downhole Positive Displacement Motor Improves Reliability and Enhances Performance in 16-in Vertical Sections[J]. 2009, SPE126053 presented at SPE Saudi Arabia Section Technical Symposium and Exhibition ,May 09-11,Alkhobar.

[4] B.Guidroz , M.Hussain, D. Erlandson, etal. Unique Motor Design Decreases Costs While Improving Performance in High Speed Drilling Applications [J].2013, SPE/IADC163409 presented at SPE/IADC Drilling Conference and Exhibition, Mar 05-07, Amsterdam.

[5] M.S.Kim. G.S.Lee .S.Y.Jung, etal. Design of Rotor for Internal Gear Pump Using Cycloid and Circular-Arc Curves[J]. Journal of Mechanical Design,2012,134:0110051-01100511
[6] Pat Herbert. Drilling With New-Generation Positive Displacement[A].SPE 10239, 1981.
[7] Litvin. Gear Geometry and Applied Theory[M]. New Jersey: PTR Prentice Hall,1994:1-10.
[8] J.E.Board ,A.S.Hall , W.Soedel .Comparison of Hypotrochoidal and Epitrochoidal Gerotors[J]. Journal of Mechanical Design,1991,113:133-141.
[9] A.J.Shih . Analysis and Comparison of Epicycloidal and Hypocycloidal Internal Combustion Engine Mechanisma[J]. Transactions of the ASME,1993,115:960-966.
[10] A.J.Shih .Kinematics of the Cycloidal Internal Combustion Engine Mechanism[J]. ASME Journal of Mechanical Design,1993,115(4):953-959.
[11] Kamran, Z.Mirza. The Progressing Cavity Pump:A Cost-Effective Multiphase Transfer Solution [J].1997, SPE39078 presented at the Fifth Latin American and Caribbeen Petroleum Engineering Conference and Exhibition, 30August-3September, Rio de Janeiro